High frequency acoustic for nanostructures wetting characterization

Sizhe Li, Sébastien Lamant, Julien Carlier, Malika Toubal, Pierre Campistron, Xiumei Xu, Guy Vereecke, Vincent Senez, V. Thomy, Bertrand Nongaillard

High-Frequency Acoustic for Nanostructure Wetting Characterization

Sizhe Li,*[,†] Sebastien Lamant,[‡] Julien Carlier,*[,†] Malika Toubal,[†] Pierre Campistron,[†] Xiumei Xu,[§] Guy Vereecke,[§] Vincent Senez,[‡] Vincent Thomy,[‡] and Bertrand Nongaillard[†]

[†]Université de Valenciennes et du Hainaut-Cambrésis, Institute of Electronics, Microelectronics and Nanotechnology, IEMN, UMR 8520, Le Mont Houy 59313, France

[‡]University of Lille Nord de France, Institute of Electronics, Microelectronics and Nanotechnology, (IEMN, UMR 8520, Cité Scientifique, Avenue Poincaré BP 60069, 59652 Villeneuve d'Ascq, France

[§]IMEC, Kapeldreef 75, Leuven 3001, Belgium

ABSTRACT: Nanostructure wetting is a key problem when developing superhydrophobic surfaces. Conventional methods do not allow us to draw conclusions about the partial or complete wetting of structures on the nanoscale. Moreover, advanced techniques are not always compatible with an in situ, real time, multiscale (from macro to nanoscale) characterization. A high-frequency (1 GHz) acoustic method is used for the first time to characterize locally partial wetting and the wetting transition between nanostructures according to the surface tension of liquids (the variation is obtained by ethanol concentration modification). We can see that this method is extremely sensitive both to the level of liquid imbibition and to the impalement dynamic. We thus demonstrate the possibility to evaluate the critical surface tension of a liquid for which total wetting occurs according to the aspect ratio of the nanostructures. We also manage to identify intermediate states according to the height of the nanotexturation. Finally, ourmeasurements revealed that the drop impalement depending on the surface tension of the liquid also depends on the aspect ratio of the nanostructures. We do believe that our method may lead to new insights into nanoscale wetting characterization by accessing the dynamic mapping of the liquid imbibition under the droplet.

INTRODUCTION

The wettability of solid surfaces is governed by both the chemical composition and the geometry of a surface on the micro or nanoscale. The thermodynamic equilibrium contact angles on rough and heterogeneous surfaces are commonly described as Wenzel and Cassie−Baxter models of interaction.[1] These two models describe two possible wetting states: the Wenzel and the composite (Cassie−Baxter) regimes. In the Wenzel state, the liquid penetrates the roughness of the interface. In the Cassie−Baxter model, air is trapped in the cavities of a rough surface, resulting in a composite solid−liquid−air interface. Superhydrophobic surfaces with a contact angle (CA) higher than 150° and low contact angle hysteresis (CAH < 5°) display extremely low adhesion to water. The well-known lotus effect[2] that denotes roughness-induced superhydrophobicity and the self-cleaning abilities of biological and artificial surfaces has been adopted in various applications in many disciplines, leading to a huge number of articles for more than a decade.[3−7]

An important application of nanoscale wetting concerns nanoscale wet cleaning, drying, and patterning in the field of nanoelectronics. All of these wet processes are based on nanoscale effective wetting. As a consequence, partial imbibition (either the homogeneous partial wetting of a liquid in a semi-Wenzel state or heterogeneous wetting of a liquid in a local Wenzel or Cassie state) and the nonwetting of patterned nanostructures in nanocomponent fabrication limit chemical reactions and the efficiency of the processes. These limitations concern mainly high-aspect-ratio structures for which wetting (from its characterization, modeling, and optimization) is a challenge on the nanoscale.[8]

The existence of partial wetting states in micro or nanostructures affects etching or cleaning processes during nanoscale structure fabrication. Reliable wet cleaning of nanopatterned Si wafers is an extremely important issue in the latest nanoelectronic technologies. Compared to organic chemistry, the semiconductor manufacturing industry prefers to use aqueous chemistry with a lower cost of ownership and a greener environmental profile but a higher surface tension. The realization of the hydrophilic regime plays a crucial role here,

and the potential incomplete wetting of the nanopatterned Si surfaces could impede the applicability of the current Si technology due to the absence of reliable wet cleaning on the nanoscale.[9] This concern has gained more interest since the discovery that even hydrophilic materials can present (super)-hydrophobic properties after patterning. This effect was observed for patterned surfaces constructed from hydrogenated silicon oxycarbide (SiCOH) with feature sizes of about 150 nm[10] and for nanopillars with different aspect ratios functionalized with self-assembled monolayers.[8,11] Among the applications concerned, one can mention the adsorption behavior of surfactant during the patterning wet etching or cleaning process in the field of nanoelectronics and the self-cleaning of functional solar cell devices.[12] Wettability research on the nanoscale has promoted the development of wet pattern fabrication, especially patterned organic molecules.[13] Droplets could be deposited on a specific area of the surface in which a chemical or topographical nanoscale pattern is imposed.[14]

As a consequence, it seems necessary to evaluate the wetting properties of structured surfaces on the nanoscale and to assess the wetting heterogeneity of the surface. On one hand, the most widely used method of characterizing wetting properties that remains a reference consists of a macroscopic measurement (goniometer method) at the liquid/gas/solid triple line of the drop apparent contact angle and the contact angle hysteresis. This latter value is equal to the difference between advancing and receding apparent contact angles obtained either through the tilting or the sessile drop method.[15] From a fundamental point of view, contact angles depend only on the liquid−surface interactions in the vicinity of the contact line (i.e., at the droplet rim). But working with the same surface/liquid couple, we find that the measurement of the apparent contact angle can lead to different values according to the way that the droplet is deposited (deposition speed, flow rate used to form the droplet, applied pressure, etc.). Contact angle hysteresis permits us to define the range of possible variation of the apparent angle. It is necessary to note that this information is not directly related to the local liquid−solid interaction occurring below the drop and cannot allow us to distinguish composite states.[16] By an abuse of language, the Cassie and Wenzel states are usually defined through the contact angle measurements, in the worst case by simply indicating the apparent contact angle and in the best way by stating advancing and receding contact angles. In the latter case, it is commonly admitted that hysteresis below 10° represents a nonimpaled state at the droplet rim (Cassie state by extension) and beyond 50°, an imbibed state (Wenzel sate). But it is clear that this vision corresponds to partial reality, proving the interest in detecting real wetting heterogeneity.

On the other hand, several methods have been developed to capture, on the micro/nanoscale, the interface configuration below the drop using optical methods. Moulinet and Bartolo used reflection interference contrast microscopy (RICM) to monitor the Cassie−Wenzel transition.[17] Also, Rathgen and Mugele analyzed diffraction patterns to capture the interface deformation on a superhydrophobic silicon surface made of micrometric rectangular grooves.[18] Very recently some papers[19−21] have presented methods to characterize wetting on the nanoscale level, proving the keen interest in this fundamental physics issue. Thus, while it has been shown that these latter techniques can give reliable information on the liquid−surface interaction from the macro to the nanoscale, none of them are compatible with an in situ, real time, multiscale (from macro to nanoscale) characterization.

Acoustic methods have been known for long time to allow bulk material investigation and interface characterization and make it possible to localize embedded defects in depth using the time-of-flight of the acoustic wave. The main common application concerns nondestructive evaluation such as defect characterization and adhesion evaluation. The investigation of biological tissue is commonly performed using acoustic echography. Among its advantages and using the different types of acoustic waves (bulk acoustic waves, BAW, or surface acoustic waves, SAW), authors usually highlight a nondestructive method not requiring a transparent surface and sensitivity to detect thin films at the interfaces. Depending on the type of acoustic wave, transducers can be placed either on the same side of the interface to be characterized (SAW) or on the opposite face (BAW). In the field of acoustics, only a few methods were used to characterize the wetting configuration on microstructures. To the best of our knowledge, the only case concerned roughness (phononic crystals) characterization rather than the roughness/fluid interaction. Roach et al. observed different quartz crystal microbalances (QCM) responses[22] for the penetrating and nonpenetrating liquid states. This method has shown the possibility to characterize wetting on polymer-based microstructures. Interesting results have been obtained by Paumet et al. regarding ultrasonic transmission evaluation modeling in a lower frequency range (MHz) to characterize microstructure wetting states (using a nonintegrated method in which the transducers are not directly coupled to the chip).[23] We have already demonstrated the potential of a high-frequency acoustic method for detecting wetting states on micropatterned silicon surfaces[24] and also for tracking wetting transitions on these microstructures.[25]

In this paper we present for the first time a high-frequency (1 GHz) acoustic wave echography principle to determine the wetting of a droplet on a silicon nanopatterned surface. Surprisingly our results indicate that the wetting state (in either the Cassie or Wenzel state) of a droplet placed on this type of superhydrophobic surface can be determined, even if its roughness dimensions are far below the acoustic wavelength. This technique is also highly sensitive for tracking wetting transition dynamics (partial impalement before reaching a fully imbibed state) in the nanoscale range. Moreover a comparison to classical goniometric methods will be presented, proving the complementarity of our method for detecting unobservable phenomena with conventional methods.

RESULTS AND DISCUSSION

Ordered arrays of nanopillars are etched into a 300 mm silicon wafer using a Lam Research 2300 Kiyo C series conductor etch system.[26] The pillar arrays are square packed with a 90 nm pitch; the pillars have a mean diameter of 43−31 nm and a height of 71−416 nm for an aspect ratio (AR, depth versus mean diameter) of 2−13 (Table 1). Measurements have been made thanks to SEM images (Figure 1). The top solid fraction

Table 1. Dimensions of the Nanopillars

aspect ratio: AR	2	3	7	13
mean diameter: d (nm)	43	43	36	31
depth: h (nm)	71	133	270	416
top solid fraction: f_s	0.17	0.18	0.13	0.13

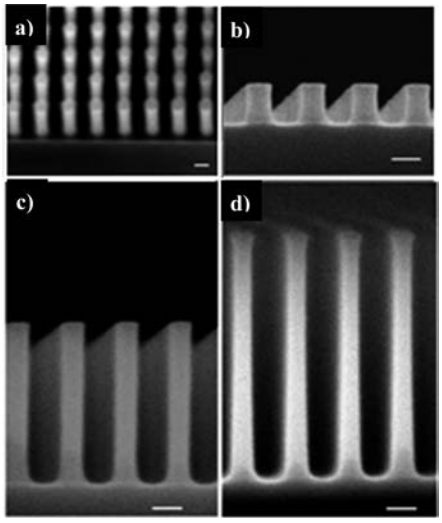

Figure 1. SEM images of the silicon nanopillars. (a) Tilted view of the square packed pillar arrays. (b–d) Cross-sectional SEM images of nanopillars with aspect ratios (ARs) of 2, 7, and 13, respectively. The scale bars are 50 nm.

f_s corresponds to the surface in contact with the liquid (top of the pillars) divided by the projected area of the surface. The calculated values vary from 0.13 to 0.17. To modify the intrinsic wettability of the nanopillars, a self-assembled monolayer (SAM) of FDTS (1*H*,1*H*,2*H*,2*H*-perfluorodecyltrichlorosilane) was grafted from the vapor phase to functionalize the silicon surface.

Wetting Characterization on Nanostructures: Goniometry as a Reference Method. The goniometric method is used to determine the wettability of the nanostructured interfaces. The tested liquids were mixtures of deionized water and ethanol (Supporting Information Table s1, section 1). The results obtained with this method will be used as references for the rest of the paper.

In order to measure the contact angle, a drop shape analysis system (DSA100, Krüss GmbH, Germany) is used, placed in clean room facilities with controlled temperature and humidity. It includes an automated dosing unit and tilting table, CCD camera (50 fps), and analysis software. A static apparent contact angle of $\theta_0^* \pm 2°$ was measured just after drop deposition (without any needle or capillary inside the droplet). Advancing and receding apparent contact angles, θ_A^* and θ_R^*, respectively, are measured using the tilting plate method: the tilting table is rotated from 0 to 90° (in steps of 2° per second), and drop deformation and displacement are recorded (50 fps, 10 computations per second) with a droplet volume equal to 8 μL. Advancing/receding apparent contact angles were calculated just before advancing/receding contact line depinning, respectively. Contact angle hysteresis (CAH) was calculated as the difference between θ_A^* and θ_R^*.

If no sliding is observed for the droplet (i.e., tilting angle of 90° with no sliding), then hysteresis cannot be determined but it indicates the impalement of the liquid, at least at the triple-phase line, corresponding to a local Wenzel state.

The tested liquids are mixtures of deionized water and ethanol. Volume proportions along with corresponding surface tensions γ are reported in Table 2. The use of such mixtures enables the easy tuning of γ while avoiding large variations in viscosity η and density ρ. The drop volume was fixed at 8 μL for all experiments. This ensures easy droplet sliding upon

Table 2. Surface Tensions of DI Water/Ethanol Mixtures (Vol %) Measured Using the Pendant Drop Method (Averaged over Five Measurements)

liquid	γ (mN/m)
DI water 100 (%)	72.6
DI water + eth 95/5 (%)	58.7
DI water + eth 90/10 (%)	52.0
DI water + eth 85/15 (%)	46.0
DI water + eth 80/20 (%)	42.9
DI water + eth 75/25 (%)	40.0
DI water + eth 70/30 (%)	35.0
DI water + eth 60/40 (%)	31.1
DI water + eth 50/50 (%)	29.2
DI water + eth 40/60 (%)	27.9

tilting while keeping the drop radius (~1 mm) slightly below the capillary length (depending on the ethanol concentration). For the apparent contact angle computation, part of the drop profile which lies near the contact line is adapted to fit a polynomial function. Apparent contact angles are then determined from the slope at the triple point. This method avoids measurement errors due to drop shape deformation under gravity.[27] For each surface–liquid set, apparent contact angles are averaged over five measurements. Then the standard deviation is also calculated.

It is to be noted that contact angle measurements were performed within approximately10 s to avoid the influence of the evaporation phenomenon. (During this short time, the surface tension of the mixture is not expected to increase more than 1 mN/m, which corresponds to a 2 to 4% error.) When the hysteresis is measured, the measurement takes less than 30 s (tilting angle inferior to 50°).

Typical evolutions of the contact angle measurements are presented in Figures 2 and 3. Using the tilting plate method, we

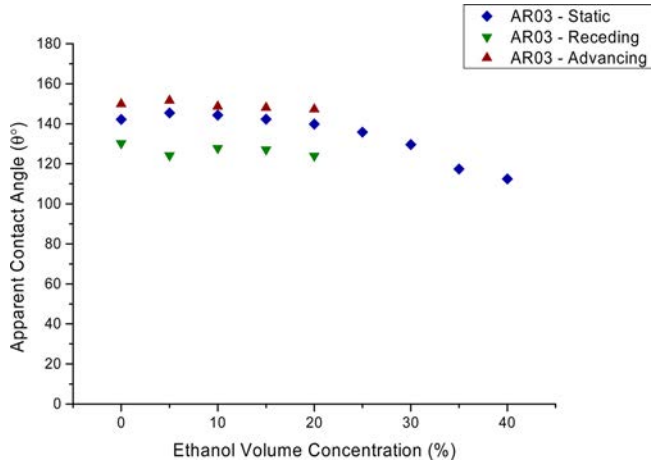

Figure 2. Ethanol/water mixture wetting on nanoscale-patterned structures with an aspect ratio of 3.

find that the advancing contact angles are equal to 150° for an ethanol concentration lower than 20% on the AR3 surface. For these same liquids, receding angles are comprised between 130 and 124 ± 2°, leading to a CAH inferior to 25 ± 2°. Once the concentration is higher than 20%, the tilting method leads to the pinning of the droplet even for a tilting angle of 90° as detailed in Figure 2. At this point, no hysteresis can be measured.

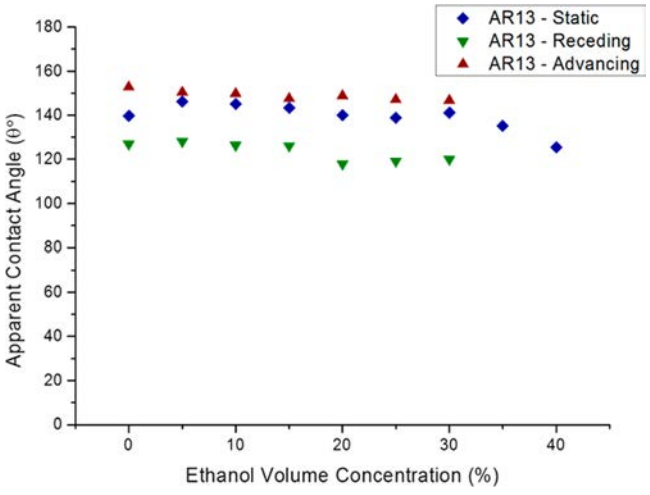

Figure 3. Ethanol/water mixture wetting on nanoscale-patterned structures with an aspect ratio of 13. Advancing and receding angles are determined by the tilting plate method. Beyond an ethanol concentration of 30%, these angles cannot be determined due to droplet pinning even for a tilting angle of 90°.

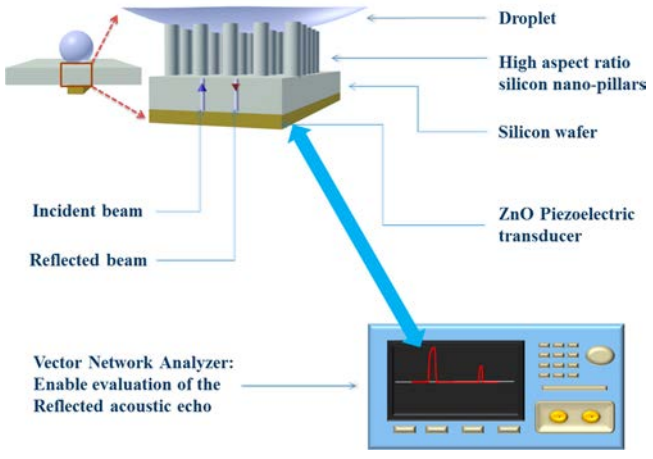

Figure 4. Acoustic method principle for the detection of both Cassie–Baxter and Wenzel wetting states: the insets show a magnified illustration of the interface between droplets and nanopillars. The vector network analyzer (VNA) is connected to the ZnO piezoelectric transducer in order to measure its electrical impedance. This transducer generates the acoustic wave incident at the interface in order to sense liquid imbibition.

On the AR13 surface, a value of 150 ± 2° is obtained for liquid presenting an ethanol concentration lower than 30% (Figure 3). At 35%, this value slightly decreases to reach 120 ± 2° at 40%. As stated before, such information is not sufficient to describe the wetting state of the droplet on a rough surface. Contact angle hysteresis measurements were then made. These results obtained on AR13 surfaces are summarized in Figure 3.

Using the tilting plate method, the advancing contact angles are equal to 148 ± 2° for an ethanol concentration lower than 30% on the AR13 surface. For these same liquids, receding angles are comprised between 130 and 123 ± 2°, leading to a CAH lower than 23 ± 2°. Once the concentration is higher than the critical concentration of 30%, the tilting method led to a pinning of the droplet even for a tilting angle of 90°: because there is no triple line movement, determinations of the advancing and receding angles are not possible.

Wetting characterization on a rough surface, by a goniometer method, of both of these surfaces led to the determination of a critical ethanol volume concentration beyond which the droplet rim is definitely impaled inside the nanostructuration. This critical value is dependent on the height of the structures, given as 35 and 25% for AR13 and AR3 respectively. According to the usual denomination adopted by the scientific community, we can assert that below this critical volume concentration a Cassie state is maintained while beyond a Wenzel state is obtained. Details of the level of impalement and of the dynamic of imbibition cannot be determined through this goniometric method.

Acoustic Measurements on Nanostructured Surfaces. This method is based on the high-frequency echography principle. It consists of the evaluation of the reflection of a high-frequency (1 GHz) longitudinal wave on a patterned interface. Depending on the wettability of these structures, the reflection/transmission coefficients are modified.

The acoustic reflection coefficient is deduced from the measurement of the electrical impedance of the ZnO piezoelectric transducer placed on the back side of a superhydrophobic silicon surface (Figure 4). These transducers are fabricated thanks to ZnO sputtering on the back side of the wafer. A ground layer is first deposited on the substrate (Ti/Pt: 10/100 nm). After a lithography step, a layer of 2.4 μm of ZnO is sputtered and a layer of 100 nm of Pt is evaporated to achieve the top electrode. The transducers are then obtained thanks to the classical lift-off technique. The transducers have a central resonance frequency of 1 GHz with a 3 dB bandwidth of about 800 MHz.

The power applied to the transducer via the vector network analyzer is 0 dBm. Because the excitation wave is a longitudinal wave (compression mode), there is almost no flexural plate or torsion mode that is excited. We have calculated the resonance frequency for the compression mode (clamped pillar) of the highest nanopillars, which is in the range of 5 GHz (the quarter wavelength should be equal to the height of the AR13 nanopillars) that is out of the bandwidth of the measurement. As a consequence, with an incident power of 1 mW (from which electrical and electromechanical losses have to be withdrawn), there is no influence on the wetting phenomena.

The transducer is used to generate the acoustic wave incident at the interface. The S_{11} scattering parameter (ratio of the complex amplitudes of the reflected and incident signals) is measured using a SussMicrotech probe coupled with a Rohde & Schwarz 300 kHz–8 GHz vector network analyzer. Then an inverse Fourier transform is applied to the $S_{11}(f)$ signal to process the reflected echoes in the time domain. The amplitude of the measured signal is normalized to air in order to remove the intrinsic insertion losses from measurements.

These reflected waves have been modeled and confirmed through experimental results on microstructures.[24] The feasibility of following the evolution of the wetting state in various experiments (electrowetting on dielectric, evaporation) has also been demonstrated in previous work.[25] On microstructures, two reflection coefficients can be observed at the top and bottom of the microstructures. (In the case of high-frequency acoustic characterization, the frequency bandwidth of the transducers makes it possible, in the time domain, to separate the echoes reflected on top and bottom interfaces.) It is possible to evaluate the presence of liquid above the

microstructures or between the microstructures if the liquid is in direct contact with the bottom interface.

In the case of nanostructures, the acoustic wave interaction with the solid is different due to the fact that the structural dimensions are much smaller than the longitudinal bulk acoustic wavelengths (at 1 GHz about 8.5 and 1.5 μm in silicon and water, respectively). The incident wave on the nanostructured interface generates a vibrational state of the nanopillars modified by the different wetting state. Thus, according to the nanostructures' imbibition, this nanostructured interface presents an equivalent mechanical impedance modifying the reflection coefficient.

The reflection coefficient is the one normalized with respect to air. From a theoretical point of view, considering a plane acoustic wave propagating at normal incidence onto an interface separating two media of mechanical acoustic impedances Z_1 and Z_2, the absolute value of the reflection coefficient $R_{2/1}$ can be calculated from the following equation:

$$|R_{1/2}| = (Z_2 - Z_1)/(Z_1 + Z_2) \quad (1)$$

$Z = \rho v$, with ρ being the density of the medium and v being the acoustic velocity of the wave propagating inside. (As a first approximation, only the real part of the mechanical impedance is considered.) In our case, Z_2 is the acoustic impedance of the liquid and Z_1 is the acoustic impedance of the (100) silicon substrate.

In order to characterize the wetting properties of the nanostructured interface, the evaluation of the acoustic reflection coefficient will be achieved using liquids of known acoustic properties. Ethanol/water mixtures, which make it possible to modify the surface tension of a liquid, will first be characterized on nonpatterned substrates so as to calibrate the acoustic method. Then the wettability of the nanostructured surfaces will be studied using the same mixtures.

To understand the physical significance of reflection coefficient R, eq 2 describes the influence of the different parameters on our measurements.

$$R = R_{Si/w}A_{cw} + R_{Si/air}(1 - A_{cw}) \quad (2)$$

where $R_{Si/W}$ is the reflection coefficient at the silicon−water interface, $R_{Si/air}$ is the reflection coefficient at the silicon−air interface, A_{cw} is the part of the area of the transducer covered by water, and $1 - A_{cw}$ is the complementary part of the area of the transducer covered by air

Thus, the reflection coefficient is a function of the part of air, liquid, and silicon in front of the transducer. The sensitivity of the method mainly depends on the high contrast between air and liquid impedances (Supporting Information)

A first set of data dealing with the acoustic characterization of the wetting on nanotextured surfaces at different ethanol concentrations is presented in Figure 5. This figure represents the evolution of the acoustic reflection coefficient on three different nanotextured surfaces presenting the same aspect ratio (AR2). The results are compared to a reference corresponding to a planar (nontextured) silicon wafer on which the surface treatment based on the use of a self-assembled monolayer (SAM) described previously was also achieved. For Figures 5 and 6, error bars indicate the general repeatability of the acoustic reflection coefficient measurement (±0.003).

In dealing with the AR2 surface, the measurement matching the ethanol concentration C = 0% corresponds to a water droplet. The experiments have been achieved using a droplet of

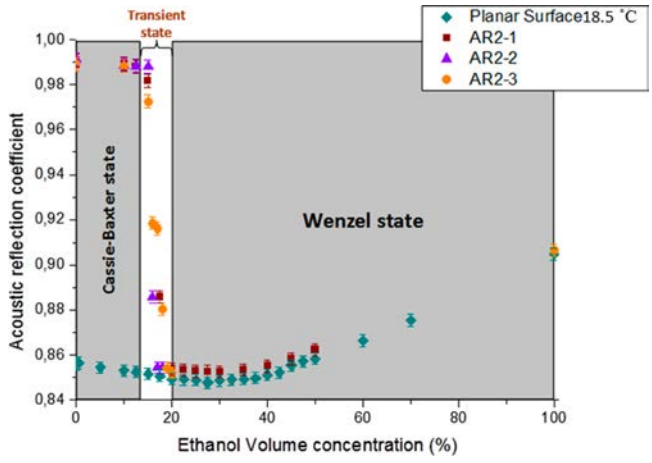

Figure 5. Acoustic reflection coefficient for different water/ethanol mixtures on planar and AR2 surfaces. For an ethanol concentration varying from 0 to 15%, a Cassie state is observed, and between 15 and 20%, the acoustic reflection coefficient decreases sharply, indicating a wetting transient state before reaching a Wenzel state for concentrations beyond 20%.

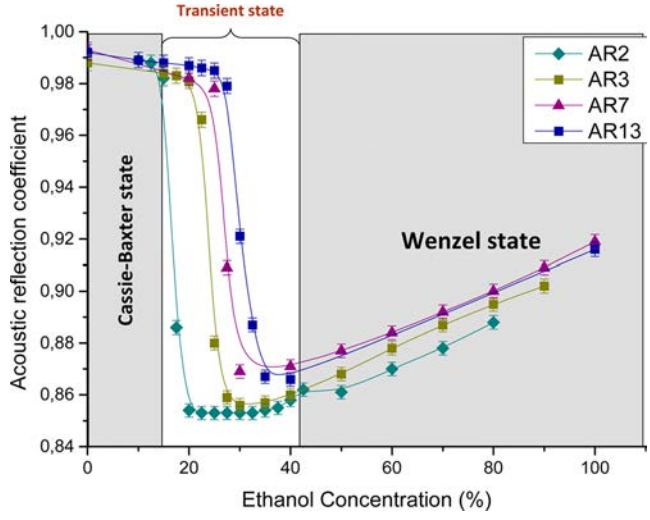

Figure 6. Acoustic reflection coefficient for different water/ethanol mixtures on different surfaces: nanostructures with aspect ratios from 2 to 13.

each ethanol-based solution prepared separately. A droplet with a known concentration has been deposited on the surface. Once the acoustic measurement was made, the structures were dried with nitrogen. Then another droplet was deposited, and operations were repeated as described previously. The droplets came from the prepared solution from lowest to highest ethanol concentration. We have chosen this order so as to obtain wetting states from Cassie−Baxter to Wenzel so as to limit surface pollution. This pollution comes from the deposition of particles present in the initial solution, regardless of the care taken in the purity of the liquid or from the particles present on the surface and deposited/concentrated on the structures. This can modify the original wetting properties of the structures. While the measurement is calibrated to obtain a value equal to 1 for a surface without any droplets, the value of the reflection coefficient on AR2 is equal to 0.99, which corresponds to the influence of liquid at the top of the pillars. Indeed, a part of the acoustic energy is transmitted to the liquid, proportionately to

the top solid fraction f_s given in Table 1. At this point it is to be noted that we can observe a slight decrease in the acoustic reflection coefficient for ethanol concentrations of up to 15% for the AR2 surface. This slope can be compared to the same evolution obtained on a planar surface: the variation of the reflection coefficient is due to the variation of the mechanical impedance of the mixture according to the ethanol concentration. The gap between the planar and the rough surface curves is explained up to this 15% concentration by the presence of air on AR2, revealing a Cassie state. For concentrations of between 15 and 20%, a transient state is observed for which the acoustic reflection coefficient decreases rapidly from 0.99 to 0.85. This huge variation is ascribed to the increase in the area of the interface between silicon and liquid embedded inside the nanopillars under the droplet (placed in front of the transducer), which is modifying the reflection coefficient.

From the 20% ethanol concentration, the reflection coefficient is almost the same for both AR2 and planar surface. It indicates that from an acoustic point of view, no difference can be made between the planar surface covered by a liquid droplet and the nanotextured surface covered by the same liquid droplet. Thus, a perfect contact appears between surface and liquid in both cases, revealing a total Wenzel state for the AR2 surface in front of the entire transducer surface. Finally it is to be noted that the nonmonotonous curve on the planar surface is directly linked to the classical variation of the mechanical impedance of the liquid according to the ethanol concentration (details I Supporting Information, Figure S1, section 1).[28] Moreover, evaporation, which may be critical to the water/ethanol droplet, is considered to be negligible (modification of 0.2% of the reflection coefficient) according to the duration of the experiment (10 s) (details in Supporting Information, Figure S2, section 2).

The same measurements have been achieved on different nanotextured surfaces presenting aspect ratios from 2 to 13. The results are presented in Figure 6. Compared to AR2 surfaces, for which wetting properties have already been presented, the general trend in these curves is identical. For ethanol concentrations below a certain critical value, the acoustic reflection coefficient starts from 0.99 and slowly decreases to 0.985, and then a sharp decrease is observed. Beyond this concentration value, the signal on the nanotextured surface coincides with that on the planar surface. The only difference is the critical ethanol concentration for which the reflection coefficient falls down: it is directly linked to the aspect ratio AR.

DISCUSSION

Measurements obtained by both goniometric and acoustic methods on nanotextured surfaces led to the same critical ethanol concentration for which a modification of the wetting state is assumed. At first sight, this modification is called a transition from a Cassie to a Wenzel state. Nevertheless the optical methods, considered to be the reference, do not authorize us to go further in the analysis of the Cassie−Baxter to Wenzel transition.

Indeed, from a physical point of view, it is important to underline that even if we confront two different wetting characterization techniques (goniometric and acoustic methods), the information obtained is not totally comparable. As detailed before, theoretically, contact angle hysteresis depends on the triple-phase line (not on the wetting state under the droplet), while the acoustic method is sensitive to partial impalement in the nanostructuration facing the acoustic transducer. We thus measured different wetting transitions (local/outskirt), but it seems that in our case there is not a huge difference in the critical ethanol concentration.

Nevertheless, the acoustic method presented here authorizes a deeper observation of the nanoscale wetting. It is then possible to extract some quantitative characteristics of the transition from the Cassie−Baxter to Wenzel state (C−B/W). Indeed, in Figure 6, one can observe that the evolution of the reflection coefficient shows an inflection point, at a critical ethanol concentration, which can be correlated to a transient state, from Cassie−Baxter to Wenzel in our case. By calculating the evolution of the slope of the local tangent related to each transition curve from Figure 6, we can determine the maximum of the absolute value of this slope. In Table 3 we report relevant values of the critical ethanol concentration $C_{C-B/W}$, the surface tension $\gamma_{C-B/W}$, and the maximum in the absolute value of the slope $|S_{max}|$.

Table 3. Quantitative Characterization of the Transition Curve Depending on the Aspect Ratio[a]

	AR2	AR3	AR7	AR13
$C_{C-B/W}$ (%)	17.5	25	27.5	30
$\gamma_{C-B/W}$ (mN/m)	44	39.5	38.2	36.5
$\lvert S_{max}\rvert$	0.0384	0.0344	0.0276	0.0232

[a] $C_{C-B/W}$, ethanol concentration; $T_{C-B/W}$, surface tension for which the slope of the transition curve is maximized; $|S_{max}|$, calculated value of the maximum of the absolute value of the slope of the curve.

One can conclude that the higher the aspect ratio, the higher the concentration $C_{C-B/W}$ and the lower the surface tension $\gamma_{C-B/W}$. It shows that increasing the aspect ratio will help to maintain the Cassie−Baxter state. Furthermore, $|S_{max}|$ decreases as the aspect ratio increases, revealing that the dynamics of drop impalement is strongly correlated to the nanopillar height. The impalement is all the more brusque because the aspect ratio is low.

The imbibition of the liquid in the nanostructures will thus affect the equivalent impedance at the interface, and the acoustic reflection coefficient will be modified. Furthermore, this measure is a mean value integrated over the whole transducer surface. No differentiation can be made between (i) a surface presenting a homogeneous air layer between silicon and water and (ii) a heterogeneous filling presenting both liquid/solid and solid/air/liquid mixed local states.

The interpretation of these results remains open. From the usual models applied to this type of surface, two types of impalement on vertically structured surfaces (with h being the height and l being the maximum spacing between two structures (side to side)) can be considered.

First, when high pressure is applied to the droplet, its shape between each pillar is deformed. For low pressure, the liquid/gas interface exhibits a flat profile, but for higher pressure, the curvature radius of this interface may be on the order of magnitude of the distance between pillars. In this case, depending on the height of the pillars, the liquid comes into contact with the bottom of the texturation, leading to a wetting transition from Cassie to a Wenzel state. This transition requires a high pressure of tens of bars that could not be reached in our case

Second, once the liquid contact angle is locally equal to the advancing contact angle on the wall of the microstructures, the liquid slides down the wall before reaching the bottom of the structure. The scaling law is $P_s \propto \gamma(\cos(\theta_a))/l$, with P_s being the sliding pressure and θ_a being the advancing contact angle. When the pressure becomes positive, the liquid wets the walls and then all of the structure. In this scenario, the re-entrant angle at the top of the structure according to the height of the nanopillars can affect the wettability properties of the textured surface (as an interesting result, the realization of a superoleophobic surface from an oleophilic material is achievable with reentrant structures[28]), and P_s becomes $\gamma(\sin(\theta_a))/l$. But according to SEM pictures given in Figure 1, this is not the case with the surfaces under investigation in this paper.[10]

The transition from Cassie to Wenzel appears when the lower of the two pressures P_i and P_s is reached.

Another possible explanation has recently been proposed by Xu et al.[10] They evidence, thanks to an original optical reflectance method, that during the nanofabrication process (exposure of different crystallographic planes, nanoroughness from etching, and perturbation of SAMs packing on a curved surface) a lowering of the surface energy of pillar sidewalls appears, as compared to a planar (1 0 0) silicon wafer surface. They used water droplets combined with a large number of different SAMs presenting various surface energies. In the present study, a unique SAM is used, and the liquid surface tension varies by adding ethanol to water (Figure 5). We thus obtain, on identical surfaces, the same impalement behavior whatever the studied parameter (surface energy of the surface or surface tension of the liquid) characterized by three different methods: an original optical reflectance method (Xu et al) and, in this paper, a goniometric method and an original high-frequency acoustic method. A representation of our acoustic measurements against the Young's angle on a silicon planar surface (that can be easily deduced from Figure 6 where the representation is achieved against the ethanol volume concentration) would show a deviation in the transition criteria of more than 20° compared to classical models, similar to the observations of Xu et al.[11] on the same structures achieved by an optical reflectance method. This shows a coherent wetting transition observation for different aspect ratios using three different methods (acoustic, optical reflectance, and goniometry).

CONCLUSIONS

Goniometric optical methods make it possible to evaluate the wetting of a droplet on nanostructures, but this characterization is limited to the droplet rim, where the triple line is defined. On the micro/nanoscale, the liquid/solid/gas interface can be characterized by different methods to huge accuracy, but none of them are compatible with an in situ, real time, multiscale (from macro to nanoscale) characterization. For the first time, a high-frequency acoustic method has been proposed to evaluate the wetting phenomena locally on nanostructures. This acoustic method has shown its extreme sensitivity to the level of liquid imbibition. It was then possible to demonstrate the possibility of evaluating the ethanol concentration of a liquid for which total wetting can be obtained depending on the aspect ratio of the nanostructures. As an example, it was possible to demonstrate that the total wetting of nanostructures with an aspect ratio of 13 (AR13) was obtained for an ethanol concentration equal to 30% (surface tension of 29 mN/m) whereas for nanostructures with an aspect ratio of 2 (AR2), the total wetting was observed for a concentration of 20% (surface tension of 43 mN/m).

Beyond these results, it is important to underline the potential of our acoustic method. Among the different advantages, this method allows us to characterize the wetting under the droplet where the goniometer method cannot give any information. By lowering the transducer diameter, we believe that we will be able to evidence partial wetting imbibition and temporal evolution of the imbibition. Moreover, the integration of these smaller transducers in the network may lead to a mapping of the wetting under the droplet. Finally, independently of the triple line (rim of the droplet) our acoustic method can characterize the solid/liquid film, in particular, the local concentration of a mixture during evaporation processes or particle sedimentation during wet cleaning processes.

ASSOCIATED CONTENT

Supporting Information

Validation of the acoustic characterization method. Evaporation effect quantification. This material is available free of charge via the Internet at http://pubs.acs.org.

AUTHOR INFORMATION

Corresponding Authors

E-mail: lisizhe1987@163.com.

E-mail: julien.carlier@univ-valenciennes.fr.

Author Contributions

Sizhe Li and Sebastien Lamant contributed equally to this article and are first coauthors.

Notes

The authors declare no competing financial interest.

ACKNOWLEDGMENTS

This work is supported by the Nord-Pas-de-Calais Region through the 2008−2013 CIA and CISIT State Region Planning contracts and by the French Agence Nationale de la Recherche (ANR) under reference Reflex ANR-11-NANO-0007.

REFERENCES

(1) Lafuma, A.; Quere, D. Superhydrophobic states. *Nat. Mater.* **2003**, *2*, 457.

(2) Barthlott, w.; Neinhuis, C. Purity of the sacred lotus, or escape from contamination in biological surfaces. *Planta* **1997**, *202*, 1−8.

(3) Herminghaus, S. Roughness-induced non-wetting. *Europhys. Lett.* **2000**, *2*, 165−170.

(4) Marmur, A. From hygrophilic to superhygrophobic: theoretical conditions for making high-contact-angle surfaces from low-contact-angle materials. *Langmuir* **2008**, *24*, 7573−7579.

(5) Bocquet, L.; Lauga, E. A smooth future ? *Nat. Mater.* **2011**, *10*, 334−337.

(6) Tuteja, A.; Choi, W.; Ma, M. L.; Mabry, J. M.; Mazzella, S. A.; Rutledge, G. C.; McKinley, G. H.; Cohen, R. E. Designing Superoleophobic Surfaces. *Science* **2007**, *318*, 1618−1622.

(7) Kwon, Y.; Choi, S.; Anantharaju, N.; Lee, J.; Panchagnula, M. V.; Patankar, N. A. Is the Cassie-Baxter formula relevant? *Langmuir* **2010**, *26*, 17528−17531.

(8) Xu, X. M.; Vereecke, G.; van den Hoogen, E.; Smeers, J.; Armini, S.; Delande, T.; Struyf, H. Wetting Challenges in Cleaning of High Aspect Ratio Nano-Structures. *Solid State Phenom.* **2012**, *195*, 235−238.

(9) Mrsella, J. A.; Durham, D. L.; Molnar, L. D. In *Handbook of Cleaning for Semiconductor Manufacturing*; Reinhardt, K. A., Reidy, R.

F., Eds.; Wiley and Scrivener Publishing LLC: Salem, MA, 2003; p 565.
(10) Harder, P. M.; Schedd, T.A.; Colburn, M. Static and Dynamic Wetting Characteristics of Nano-patterned Surfaces. *J. Adhes. Sci. Technol.* **2008**, *22*, 1931.
(11) Xu, X. M.; Vereecke, G.; Chen, C.; Pourtois, G.; Armini, S.; Verellen, N.; Tsai, W.-K.; Kim, D.-W.; Lee, E.; Lin, C. Y.; Van Dorpe, P.; Struyf, H.; Holsteyns, F.; Moshchalkov, V.; Indekeu, J.; De Gendt, S. Capturing Wetting States in Nanopatterned Silicon. *ACS Nano* **2014**, *8*, 885−893.
(12) Weiwei, W. Surface Engineering Method to Fabricate a Bendable Self-Cleaning Surface with High Robustness. *Sci. Adv. Mater.* **2013**, *5*, 1−6.
(13) Joachim, C.; Gimzewski, J. K.; Aviram, A. Electronics using hybrid-molecular and mono-molecular devices. *Nature* **2000**, *408*, 541.
(14) Aronov, D.; Molotskii, M.; Rosenman, G. Electron-induced wettability modification. *Phys. Rev. B: Condens Matter* **2007**, *76*, 035437.
(15) Marmur, A. The Lotus Effect: Superhydrophobicity and Metastability. *Langmuir* **2004**, *20*, 3517.
(16) Gao, L.; McCarthy, T. J. Wetting 101°. *Langmuir* **2009**, *25*, 14105.
(17) Moulinet, S.; Bartolo, D. Life and death of a fakir droplet: Impalement transitions on superhydrophobic surfaces. *Phys. J. E* **2007**, *24*, 251.
(18) Rathgen, H.; Mugele, F. Microscopic shape and contact angle measurement at a superhydrophobic surface. *Faraday Discuss.* **2010**, *146*, 49.
(19) Papadopoulos, P.; Mammen, L.; Deng, X.; Vollmer, D.; Butt, H. J. How superhydrophobicity breaks down. *Proc. Natl. Acad. Sci. U.S.A.* **2013**, *110*, 3254.
(20) Rykaczewski, K.; Landin, T.; Walker, M.; Scott, J. H.; Varanasi, K. K. Direct Imaging of Complex Nano-to Microscale Interfaces Involving Solid, Liquid, and Gas Phases. *ACS Nano* **2012**, *6*, 9326.
(21) Paxson, A. T.; Varanasi, K. K. Self-similarity of contact line depinning from textured surfaces. *Nat. Commun.* **2013**, *4*, 1.
(22) Roach, P.; McHale, G.; Evans, C. R.; Shirtcliffe, N. J.; Newton, M. I. Decoupling of the Liquid Response of a Superhydrophobic Quartz Crystal Microbalance. *Langmuir* **2007**, *23*, 9823.
(23) Paumel, K.; Moysan, J.; Chatain, D.; Corneloup, G.; Baque, F. Modeling of ultrasound transmission through a solid-liquid interface comprising a network of gas pockets. *J. Appl. Phys.* **2011**, *110*, 044910.
(24) Saad, N.; Dufour, R.; Campistron, P.; Nassar, G.; Carlier, J.; Harnois, M.; Merheb, B.; Boukherroub, R.; Senez, V.; Gao, J.; Thomy, V.; Ajaka, M.; Nongaillard, B. Characterization of the state of a droplet on a micro-textured silicon wafer using ultrasound. *J. Appl. Phys.* **2012**, *112*, 104908.
(25) Dufour, R.; Saad, N.; Carlier, J.; Campistron, P.; Nassar, G.; Toubal, M.; Boukherroub, R.; Senez, V.; Nongaillard, B.; Thomy, V. Acoustic Tracking of Cassie to Wenzel Wetting Transitions. *Langmuir* **2013**, *29*, 13129−13134.
(26) Vos, I.; Hellin, D.; Vertommen, J.; Demand, M.; Boullart, W. Silicon Nano-Pillar Test Structures for Quantitative Evaluation of Wafer Drying Induced Pattern Collapse. *ECS Trans.* **2011**, *41*, 189−196.
(27) Patankar, N. A. Hysteresis with regard to Cassie and Wenzel states on superhydrophobic surfaces. *Langmuir* **2010**, *26*, 7498.
(28) Vatandas, M.; Koc, A. B.; Koc, C. Ultrasonic velocity measurements in ethanol−water and methanol−water mixtures. *Eur. Food Res. Technol.* **2007**, *225*, 525−532.
(29) Dufour, R.; Perry, G.; Harnois, M.; Coffinier, Y.; Thomy, V.; Senez, V.; Boukherroub, R. From micro to nano re-entrant structures: Hysteresis on superomniphobic surfaces. *Colloid Polym. Sci.* **2013**, *291*, 409−415.